GATING CURRENT HARMONICS

IV. Dynamic Properties of Secondary Activation Kinetics in Sodium Channel Gating

JURGEN F. FOHLMEISTER*‡ AND WILLIAM J. ADELMAN, JR‡
*Laboratory of Neurophysiology, University of Minnesota, Minneapolis, Minnesota 55455; and
‡Laboratory of Biophysics, IRP, National Institute of Neurological and Communicative Disorders and Stroke, National Institutes of Health at the Marine Biological Laboratory, Woods Hole, Massachusetts 02543

ABSTRACT The kinetics for sodium channel gating appear to involve three coupled processes: (*a*) "primary" activation, (*b*) "secondary" activation, and (*c*) inactivation. Gating current data obtained in dynamic steady states with sinusoidal voltage-clamp were analyzed to give further details about the secondary activation process in sodium channel gating. Unlike primary activation and inactivation, the secondary activation kinetics involve physical processes that become defined when the data are analyzed as a function of the sinusoid frequency in addition to mean membrane potential. The effects of these processes are described, and a physical interpretation is presented.

INTRODUCTION

Three earlier papers (Fohlmeister and Adelman, 1985*a*, *b*, 1986) develop quantitatively the kinetics of sodium channel gating from gating current data obtained in sinusoidally driven dynamic steady states. Of the observed three kinetic processes, the description of the "secondary activation kinetics" was left incomplete. This communication completes the description from the viewpoint of dynamic steady-state data.

MATERIALS AND METHODS

Details of squid axon experiments and computer simulation procedures were the same as those given in Fohlmeister and Adelman, 1985*a* (Methods).

NEAR OPTIMIZATION OF MODEL PARAMETERS

Secondary activation gating is modelled as a first order kinetic process $x_0 \rightleftharpoons x_6$, whose rate constants

$$k_{06}(x_i, E) = \frac{x_1 + x_2 + x_3 + x_4}{x_1 + x_2 + x_3 + x_4 + x_5} \kappa_{06}(E) \qquad (1a)$$

$$k_{60}(x_i, E) = \frac{x_5}{x_1 + x_2 + x_3 + x_4 + x_5} \kappa_{60}(E) \qquad (1b)$$

depend on the states x_i, $i = 1...5$, occupied by the primary activation mechanism, and on membrane potential, E. The coupling between the secondary and primary processes is given by the fractions containing the x_i in Eq. 1. This coupling is strong, and strictly independent of command frequency, and constitutes the principal motive force for transitions in the secondary activation gating mechanism. (The coefficients of κ_{06} [and κ_{60}] vary from nearly one [zero] to nearly zero [one], respectively, after a depolarization from −60 to 0 mV). Nevertheless, because charge movements are associated with the secondary process, its rate constants contain a direct, if relatively weak, voltage-dependence. The voltage-dependent factors of those rate constants were determined to be

$$\kappa_{06} = 200 \exp(0.016E) \qquad (2a)$$

$$\kappa_{60} = 200 \exp(-0.016E) \qquad (2b)$$

(Fohlmeister and Adelman, 1985*b*, Eqs. 7a and 7b), where the coefficients, 200, have units of inverse milliseconds, and E is the membrane potential in millivolts.

Further analysis of the model has shown that the simultaneous variation of two parameters results in an improved fit to the dynamic steady state data: The first parameter change is an offset of +20 mV in the membrane potential for which κ_{06} and κ_{60} are equal, thus

$$\kappa_{06} \rightarrow 200 \exp[0.016(E + 20)] \qquad (3a)$$

$$\kappa_{60} \rightarrow 200 \exp[-0.016(E + 20)]. \qquad (3b)$$

Correspondence should be addressed to Dr. Jurgen F. Fohlmeister.

This shift removes the remaining differences between model and data in the shape of the curve of the normalized amplitude of the second harmonic as a function of E_{mean} when inactivation gating is included (Fig. 1 *A*; cf. also Fohlmeister and Adelman, 1986, Figs. 4 and 7). Significantly, it also improves the fit of the normalized amplitude of the second harmonic in the upper E_{mean} range for activation gating kinetics alone at the higher command frequencies (Fig. 1 *B*). (Without this correction, that normalized amplitude behaves qualitatively like Fig. 2 in Fohlmeister and Adelman, 1985*b*.) However, while optimizing the shapes of the curves of the harmonic components, the entire set of model generated harmonic curves is displaced by 8 mV towards more positive membrane potentials. This latter effect is compensated with the replacement of $E \rightarrow E + 8$ in all model rate constants for both primary and secondary activation gating kinetics,and constitutes the second of the two simultaneous parameter changes. The affected equations then read:

$$a(E) = \frac{-0.07(E + 8)}{\exp[-0.07(E + 8)] - 1} \quad (4a)$$

$$b(E) = \exp[-0.04(E + 8)] = 0.726 \exp[-0.04E] \quad (4b)$$

(cf. Fohlmeister and Adelman, 1985 *b*, Eqs. 6a and 6b), and

$$\kappa_{06} = 200 \exp[0.016(E + 28)] = 313 \exp(0.016E) \quad (5a)$$

$$\kappa_{60} = 200 \exp[-0.016(E + 28)] = 128 \exp(-0.016E) \quad (5b)$$

(cf. Fohlmeister and Adelman, 1985 *b*, Eqs. 7a and 7b).

FREQUENCY DEPENDENCE OF SECONDARY ACTIVATION KINETICS

It was noted in Fohlmeister and Adelman (1985*b*) that the direct voltage dependence of the secondary activation rate constants appears to "weaken" as the command frequency is increased. The principal indication for this lies in the changing slope of the experimental curve of the normalized amplitude of the second harmonic as a function of E_{mean}, whose peak increases in value and becomes more spiked when the command frequency is increased (compare Fohlmeister and Adelman, 1985*a*, Figs. 7 and 9). Simulations with the kinetic model clearly show that this particular changing shape can only be reproduced by altering the voltage response of the secondary activation rate constants, and show further that all other model parameters must be held unchanged as the command frequency is varied.

The dynamic steady-state data are satisfied for all frequencies, f, with the following rate constants

$$\kappa_{06}(f) = 313 \exp[0.016(E_{mean} + g(f)E_{sin})] \quad (6a)$$

$$\kappa_{60}(f) = 128 \exp[-0.016(E_{mean} + g(f)E_{sin})] \quad (6b)$$

with the units of E_{mean} and E_{sin} in millivolts, those of the numerical factors ± 0.016 in mV^{-1}, and $g(f)$ a dimensionless function of frequency f. As indicated, the direct voltage-dependence remains unchanged so far as the level of E_{mean} is concerned. The frequency dependence is confined to the response to the voltage-sinusoid, which is parametrized as the two exponential terms $0.016g(f)\,E_{sin}$ and $-0.016g(f)E_{sin}$. The factor E_{sin} represents the experimental sinusoidal component of the membrane potential

$$E_{sin}(t) = 35 \sin(2\pi ft), \quad (7)$$

unchanged in both amplitude (35 mV) and phase. The observed weakening is given by the phenomenological function $g(f)$. This function is real (that is, it introduces no phase shift), and declines from a value of one for frequencies $f \leq 600$ Hz, towards zero as the command frequency is increased (Fig. 2). Despite the experimental uncertainties in the precise shape of this function, $g < 0.1$ at 3 kHz, and may well be zero at 3 kHz and higher command frequencies.

From the point of view of physical interpretation the most important element of the parametrization in Eqs. 6a and 6b is that the function $g(f)$ gives a weakening of the rate constants' response to the voltage sinusoid without introducing a phase delay in that response. To be quite certain that no phase delay is involved, model simulations were carried out with various low pass filters including simple differential equations of the form

$$\dot{\kappa}_{06} = -1/\tau[\kappa_{06} - 313 \exp(0.016E)] \quad (8a)$$

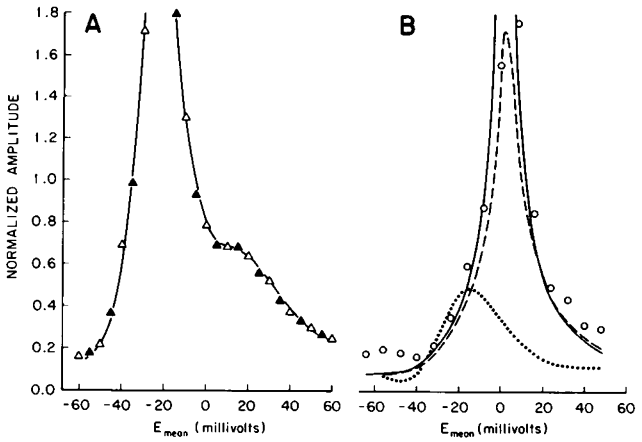

FIGURE 1 Normalized amplitudes of the second harmonic contained in dynamic steady state gating current records as functions of E_{mean}. Normalization is defined as the ratio of the second harmonic to the fundamental component at each E_{mean}. The curves give model generated normalized amplitudes with model parameters given in the text. (*A*) Normalized amplitude for the full kinetics, including inactivation gating, for f = 0.94 kHz with $g(f)$ = 0.865. Data points are from two axons identified by open and closed symbols (cf. Fig. 2). (*B*) Normalized amplitude for activation gating kinetics alone, for f = 3 kHz. *Solid curve*, $g(f)$ = 0; *dashed curve*, $g(f)$ = 0.1; *dotted curve*, $g(f)$ = 1 (see text). Data points are redrawn from Fohlmeister and Adelman, 1985*a*, Fig. 9. Normalized amplitude of the second harmonic appears to be the most sensitive single yardstick for parameter determination because of its large variations. Given the basic model kinetic structure, all other harmonic components fall into place with this adjustment.

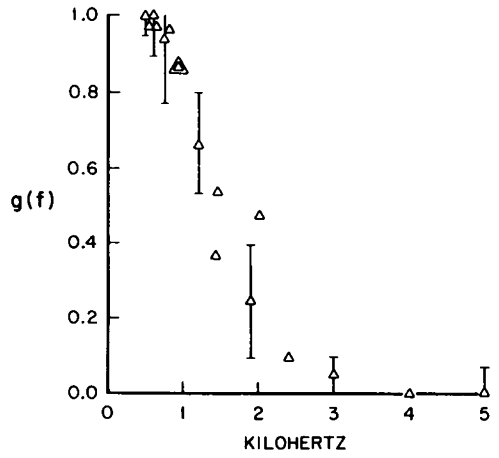

FIGURE 2 The function $g(f)$ (cf. Eqs. 6a and 6b) plotted against command frequency. The values were determined by adjusting model behavior to individual axonal data in normalized second harmonic amplitude (see Fig. 1). Error bars denote the spread when at least three axons were tested at the same frequency. Data points without error bars represent a single axon, except for the data point at 940 Hz, which represents two axons (cf. Fig. 1 *A*).

$$\dot{\kappa}_{60} = -1/\tau[\kappa_{60} - 128 \exp(-0.016E)], \qquad (8b)$$

as well as Bessel, and multipole filters with known time delays. All of these simulations led to grossly distorted harmonic curves (as compared with data), and the distortion was directly traceable to the delays introduced in the temporal variations of $\kappa_{06}(t)$ and $\kappa_{60}(t)$ by the filtering process. The absence in the experimental data of the natural time delays introduced by low pass filtering presents a challenge to physical interpretation of those data. It appears to imply at least the following two conclusions:(*a*) The electric field established by the voltage-clamp is "instantly" sensed by the elements of the secondary activation mechanism, and (*b*) despite the instantaneous sensation, the mechanism responds as though the field variations were smaller than they really are, at least for frequencies $\gtrsim$ 0.7 kHz.

A likely resolution of the paradox contained in these two conclusions is given in the Discussion. Here we point out that conclusion *a* implies synchronization between the voltage-dependence of the rate constants $k_{06}(E)$ and $k_{60}(E)$ (or $\kappa_{06}(E)$ and $\kappa_{60}(E)$) and the voltage-sinusoid; the associated gating current component, which is proportional to $x_0k_{06}-x_6k_{60}$, thereby appears with a phase-lead relative to the voltage-sinusoid. Such a phase-lead is the hallmark of a dielectric current, and its presence appears to rule out any significant ionic current contamination of the data.

DISCUSSION

The focus of the present communication is the analysis of dynamic steady-state data as a function of the frequency of the voltage-sinusoid. The analysis presupposes a kinetic structure (cf. Fohlmeister and Adelman, 1985*b*, 1986), and the refinements presented here support that basic structure while describing an unusual dynamic feature in one of its components.

The two parameter shifts made in the "Optimization" section were motivated by two observations. Without affecting any of the conclusions drawn in Fohlmeister and Adelman (1985 *a*, *b*), the new parameters (*a*) remove the remaining discrepancy between model and dynamic data for axons with intact inactivation gating (see Fig. 1 *A*), and (*b*) yield an excellent fit to the fundamental component and second harmonic data at higher frequencies (see Fig. 1 *B*).

The parameter shifts have two further consequences for the temporal development of Na-ionic currents: because inactivation gating is directly coupled to the primary activation kinetics (Fohlmeister and Adelman, 1986), the 8 mV shift in Eqs. 4a and 4b will cause an 8 mV shift in the curve of $h_\infty(E)$. This shift brings the value of E for which $h_\infty(E)$ has maximum slope (in absolute value) into near coincidence with the corresponding value for the Hodgkin–Huxley model (see Fohlmeister and Adelman, 1986, Fig. 11 *A*). The shapes of the two model-generated $h_\infty(E)$ curves remain distinct, however. The parameter changes further affect the threshold behavior of simulated action potentials. But this effect is easily compensated for by reducing the model value of $\bar{g}_{Na}$. The waveform of the action potential and post impulse trajectory is only negligibly affected.

More directly related to the principal point of this communication are changes in the rate constants of the secondary activation kinetics. The first of these changes appears in the numerical coefficients in Eqs. 5 and 6. The crucial point concerning the analysis of the dynamic data lies not in the absolute size of these coefficients, but rather in their ratio: 313/128 = 2.45. The coefficients 313 ms^{-1} and 128 ms^{-1} could each be changed by ± 50% of these values while remaining within experimental error, provided however that their ratio of 2.3 to 2.6 is maintained. The low sensitivity to absolute size of κ_{06} and κ_{60} is because that size is two orders of magnitude larger than the experimental command frequencies. An accurate determination of these relatively large coefficients would require command frequencies more nearly comparable to their size, say 50 kHz.

Finally, the two conclusions near the end of the "Frequency Dependence" section present the paradox of apparent instantaneous, but specifically erroneous sensation of the transmembrane electric field components that vary at high frequencies. It seems to us that the resolution of this paradox must involve the recognition that the data were obtained in dynamic steady states, that is, that the system has settled into a recurrent pattern. So long as that pattern is not disrupted, the system can behave in an anticipatory fashion, that is, the absence of a response delay is not inconsistent with the otherwise expected delay between cause and effect. A possible scenario is as follows: During the dynamic transient that follows the onset of the voltage

sinusoid, the secondary activation kinetics may well respond to the field change with a time delay; the waxing and waning of locally generated dipoles within the field-sensing elements of the secondary activation machinery may require a fraction of a millisecond. If the field changes with a sufficiently high frequency, $f > 1/\tau$, the response amplitude of κ_{06} and κ_{60} will be reduced, and its response will be phase shifted relative to the voltage-sinusoid (e.g., Eqs. 8a and 8b). However, as the voltage-sinusoid is continued, phase-locking forces may come into play which tend to synchronize the reduced response with the driving sine-wave. Rephrased, the system appears to find it energetically favorable to respond in a synchronous fashion. Phase-locking forces could be many. An example might be that the energy necessary for local dipole changes is most readily available at the time of maximum rate-of-change in the externally applied electric field. Thus, the maximum rates-of-change in local dipole structure and in the external field become synchronized. In the synchronized, dynamic steady state, one might then expect that the response amplitude (variations of κ_{06} and κ_{60}) might increase slightly relative to the phase shifted amplitude during the dynamic transient because of the greater energy utilization. This amplitude increase, as well as the stability of the phase-locked state, are likely to depend on the strength of the phase-locking forces, which cannot as yet be determined from our data.

Experiments were performed at the Marine Biological Laboratory in Woods Hole, MA. Computer simulations were supported in part by a grant from the University of Minnesota Academic Computing Services and Systems. J. F. Fohlmeister was supported in part through research grant BNS-8415181 from the National Science Foundation.

Received for publication 25 June 1986 and in final form 26 August 1986.

REFERENCES

1. Fohlmeister, J. F., and W. J. Adelman, Jr. 1985*a*. Gating current harmonics. I. Sodium channel activation gating in dynamic steady states. *Biophys. J.* 48:375–390.
2. Fohlmeister, J. F., and W. J. Adelman, Jr. 1985*b*. Gating current harmonics. II. Model simulations of axonal gating currents. *Biophys. J.* 48:391–400.
3. Fohlmeister, J. F., and W. J. Adelman, Jr. 1986. Gating current harmonics. III. Dynamic transients and steady states with intact sodium inactivation gating. *Biophys. J.* 50:489–502.